International Journal of Engineering & Technology, 9 (1) (2020) 69-76

International Journal of Engineering & Technology

Website: www.sciencepubco.com/index.php/IJET

Research paper

Thermal-hydraulic analysis of fuel rod of a TRIGA Mark II research reactor

Md. Shafiqul Islam [1], Abid Hossain Khan [1, 2] *

[1] *Department of Nuclear Engineering, University of Dhaka, Dhaka-1000, Bangladesh*
[2] *Department of Industrial and Production Engineering, Jashore University of Science and Technology, Jashore-7408, Bangladesh*
**Corresponding author E-mail: khanabidhossain@gmail.com*

Abstract

In this work, the feasibility of employing "Single Flow Channel Analysis" technique for obtaining the thermal-hydraulic behavior of a TRIGA Mark II research reactor has been studied. Two different simulation methods have been investigated for this purpose; one in which there is no variation in volumetric heat generation along the fuel axis and the other in which there is variation. A hot rod factor of 1.70 has been taken. Results obtained from simulation methods have been compared with both theoretical results and experimental data provided by the manufacturers. Results show that data generated from both simulation methods are more accurate compared to theoretical calculations. Also, the simulation method exempting variation of heat generation has predicted maximum temperature of the fuel centerline just above 750 ºC, which is sufficiently accurate. However, temperatures obtained at different axial and radial locations are not close to the experimental values. On the other hand, the simulation technique in which variation of heat generation exists has been able to provide temperature profiles inside the fuel rod and cladding surface almost identical to the experimental values. However, temperature profile of the fuel outer surface is found to be quite different from experimental values.

Keywords: *Hot Rod Factor; Research Reactor; Temperature Distribution; Thermal-Hydraulics.*

1. Introduction

Unlike power reactors, research reactors are specially designed nuclear reactors that are to be used for research purpose only. While power reactors produce heat energy that may be converted to useful electric energy, research reactors produce radioactive rays or particles such as neutron, α, β and γ-rays, etc. These radioactive rays and particles are used for radioactive isotope production and other research works. Heat generated during the fission chain reaction in the core is nothing but a byproduct for these reactors [1]. Research reactor fuels usually have a higher enrichment of U-235 compared to power reactors. The enrichment of U-235 is just below 20%, which is the upper limit of low-enriched uranium (LEU) fuel. In case of power reactors, this value is usually below 5%. The excess enrichment is necessary because these reactors are designed to produce maximum amount of fast neutrons, unlike power reactors that have no use of fast neutrons. Also, a massive portion of this neutron is extracted from the reactor core for research purpose. As a result, the availability of thermal neutrons is less compared to power reactors, making it difficult to sustain chain reaction at enrichment limit just below 5%. However, enrichment level above 20% is not accepted in order to avoid proliferation risks [2].

TRIGA is a pool-type reactor that is designed for research and material testing use by scientific institutions and universities. It is mostly used for undergraduate and graduate education, private commercial research, non-destructive testing, and isotope production [3]. The TRIGA reactor uses Uranium Zirconium Hydride ($U_{0.3}ZrH_{1.6}$) fuel. It has a prompt negative fuel temperature coefficient of reactivity that results in decrease in reactivity with increase in core temperature [4]. Uranium Zirconium Hydride fuels can operate at a linear heat rate (LHR) of ~80 MW/m with a maximum fuel centerline temperature of 820 ºC [5]. Another advantage of these fuels is that fission-gas release is quite small up to 600 ºC for these fuels [6]. Since these fuels do not support high temperature operation in order to avoid swelling, inert Pb-Bi-Sn liquid metal is used in between the gap of fuel pellet surface and the inner surface of the cladding instead of helium for TRIGA fuels. This modification decreases the centerline temperature of the fuel significantly [7]. Finally, the thermal conductivity of Uranium Zirconium Hydride fuel is around 20 W/m.K, which is almost 7 times higher than Uranium Oxide fuel [8]. As a result, the centerline temperature remains much lower for TRIGA reactors than conventional nuclear power plants.

TRIGA Mark-II is one of the design variations of the TRIGA research reactor types. Till date, this model is operational in multiple countries. This reactor has been used for a variety of research works and scientific studies, both experimental and numerical. Žerovnik et al. studied the use of multiple detectors on the measurement of thermal power of a TRIGA Mark II research reactor [9]. Nacir et al. worked on the safety analysis and optimization of the core fuel reloading for TRIGA Mark-II reactor in Morocco [10]. Agbo et al. analyzed the thermal power calibration methods of the Nigerian research reactor [11]. Štancar and Snoj suggested an improved thermal power calibration method for TRIGA Mark II research reactor [12]. A combined experimental and numerical study is also common in the literature for TRIGA Mark II reactors. Coupling numerical simulation techniques with research reactor experimental studies can greatly reduce the cost to be incurred during research works. Cammi et al. suggested zero-dimensional model for simulating the dynamic response of TRIGA Mark II reactor [13]. El-Bakkari et al. conducted a fuel burnup analysis for

TRIGA research reactor using Monte-Carlo nuclear code [14]. Türkmen and Çolak conducted a similar type of analysis [15]. Coban suggested a method for power level control of the TRIGA Mark-II reactor using the multi-feedback layer neural network and the particle swarm optimization [16]. Alloni et al used the Monte Carlo code for final characterization of the first critical configuration for TRIGA Mark II reactor of the University of Pavia [17]. Henry conducted a study on the physical parameters of JSI TRIGA MARK II reactor using TRIPOLI and MCNP [18]. Mghar calculated the kinetic parameters of the Moroccan TRIGA Mark-II reactor using the Monte Carlo code [19]. Cammi et al. did a characterization of the TRIGA Mark II reactor during a steady-state, full power operational condition [20]. Ćalić et al. validated the Serpent 2 code on benchmark experiments of TRIGA Mark II research reactor [21]. Henry et al. suggested a CFD/Monte-Carlo neutron transport coupling scheme applicable for TRIGA reactor [22].

The one and only research reactor in Bangladesh is the 3 MW TRIGA Mark II research reactor located at Atomic Energy Research Establishment (AERE), Savar, Dhaka. It was constructed and supplied by General Atomics, San Diego, California, USA. The reactor has been operational since 1986 [23]. Since the commissioning of the reactor, it has been an essential part of numerous nuclear research programs of Bangladesh Atomic Energy Commission (BAEC). Lyric et al. conducted an experimental study to obtain the optimum burnup of BAEC TRIGA research reactor [24]. Khan et al. analyzed the kinetic parameters of 3 MW TRIGA Mark-II research reactor at AERE using the SRAC2006 code [25]. Salam et al. measured the control rod reactivity and shutdown margin of the research reactor using analogue and digital I&C system [26]. Rahman et al. conducted a steady-state thermal-hydraulic analysis of the reactor [27]. Salam et al. measured the neutronic safety parameters of the reactor [28]. The study was extended later on by Hosan et al. [29]. Hoq et al. estimated Ar-41 activity concentration and its release rate from the reactor [30].

From the literature survey, it is evident that there have been quite a number of researches related to TRIGA Mark II research reactor. But to the best of the authors' knowledge, the prospect of using simulation tools for obtaining solely the thermal-hydraulic behavior of the fuel rod of this reactor might not have been studied earlier. Furthermore, the simplification of the simulation geometry by applying single flow channel analysis technique might not have been focused on with sufficient importance. In this work, an attempt has been made to find out the feasibility of using single flow channel analysis technique for simulating the thermal behavior of the fuel rod inside a TRIGA Mark II reactor core. In order to do so, the results from the simulation methods have been compared with results from theoretical analysis as well as experimental data.

2. Methodology

2.1. Governing equations for assessments of hydrodynamic characteristics

The 3MW TRIGA Mark II research reactor at AERE consists of 93 fuel elements, 6 control rods, 18 Graphite dummy elements, 1 Dry Central Trimble, 1 Rabbit Terminus and 1 neutron source. Again, the fuel rods are arranged in a hexagonal housing, which results in triangular array of the fuel rods. Fig.1 shows the arrangement of fuel rods in the core of the 3MW TRIGA Mark II research reactor at AERE, Savar. Since thermal-hydraulic simulation of such complex geometry will be very time consuming and complicated, it is more logical to go for single flow channel analysis. To do so, it is assumed that there exists a single flow channel of annular shape that has the same hydraulic diameter as that of the triangular flow channel of the reactor. The equivalent hydraulic diameter of the flow channel for triangular array (see Fig.2a) may be deduced as,

$$D_h = \frac{4A_{cross}}{\text{wetted perimeter}} = d_{clad,out}\left[\frac{2\sqrt{3}}{\pi}\left(\frac{p}{d_{clad,out}}\right)^2 - 1\right] \quad (1)$$

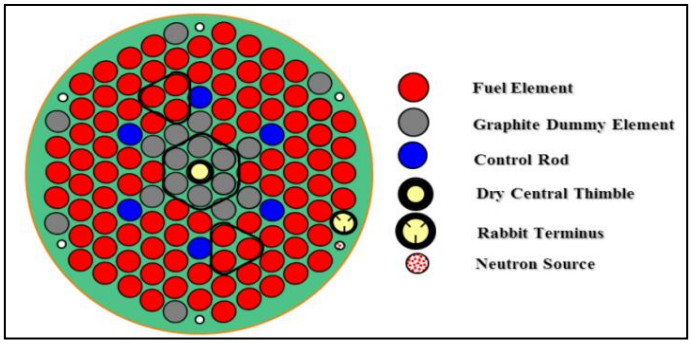

Fig. 1: Arrangement of Fuel Rods in 3MW TRIGA Mark II Reactor Core [23].

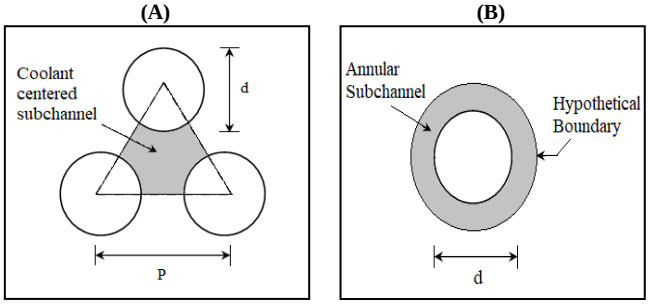

Fig. 2: A) Triangular Flow Channel, B) Annular Flow Channel.

Here $d_{clad,out}$ is cladding outer diameter, A_{cross} is cross-sectional area of flow sub-channel and p is pitch of the triangular array. For TRIGA Mark II reactor at AERE, this hydraulic diameter is calculated to be around 1.93cm.

It may be noted that for single channel flow analysis, it has be assumed that the coolant flows through an annular space between the outer surface of the cladding and a hypothetical boundary, as shown in Fig.2b. The diameter of the outer hypothetical boundary should be such that the hydraulic diameter of the annular flow channel remains the same. As a result, the diameter of the hypothetical boundary of the flow channel is calculated to be around 4.598 cm for TRIGA Mark II research reactor.

The total pressure drop across the reactor core in axial direction may be given by,

$$\Delta P_t = (P_{out} - P_{in}) = \Delta P_{friction} + \Delta P_{elev} + \Delta P_{entry} + \Delta P_{exit} \quad (2)$$

Here, $\Delta P_{friction}$ is frictional pressure drop, ΔP_{elev} is pressure drop due to elevation, ΔP_{entry} is pressure drop in the entry region and ΔP_{exit} is pressure drop at the exit region. Equation (2) may be re-written as,

$$\Delta P_t = \rho g H - \left\{f\left(\frac{H}{D_h}\right) + K_{in} + K_{out}\right\}\rho\frac{v^2}{2} \quad (3)$$

Here, ρ is density of the coolant water, H is the height of the flow channel, f is friction factor, v is velocity of the coolant and K is kinetic head loss coefficient. In case of TRIGA fuel, the cladding outer surface is very smooth. As a result, frictional head loss is very negligible. Also, pressure drop due to elevation is very small. Therefore, pressure drop observed in the flow channel is basically the sum of the pressure drops at the entry and exit location of the coolant.

2.2. Governing equations for assessments of thermal characteristics

In a nuclear power reactor, the sole purpose of the nuclear chain reaction is production of thermal energy which may be converted to electricity. On the other hand, a research reactor is designed for

producing radioactive rays and particles for research purpose. The heat produced is nothing but a byproduct and has no use whatsoever. Nevertheless, the heat energy produced in any of the two types of reactors needs to be removed from the core to avoid heating and subsequent meltdown. The rate of heat generation in a nuclear reactor may be given by,

$$\dot{q} = GN\dot{\sigma}_f V_F \varphi_{avg} \quad (4)$$

Here $\dot{q}$ is heat generation rate (W), G is energy produced per fission (J/ fission), N is number of fissionable fuel nuclei/ unit volume (atoms /cm^3), σ_f is microscopic fission cross-section of the fuel (cm^2), V_F is volume of the fuel (cm^3) and φ_{avg} is average neutron flux (n/cm^2.s) inside the core.

Unlike a power reactor, the heat produced in the core is removed by the coolant only to be dumped to the atmosphere. The rate of heat removal should, therefore, be equal to the rate of heat generation and is given by,

$$\dot{q} = \dot{m}C_{p,c}\Delta T \quad (5)$$

Here $\dot{m}$ is mass flow rate (kg/s), $C_{p,c}$ is specific heat capacity of reactor coolant (J/ kg °K) and ΔT is temperature difference across the reactor core (°C).

For most types of reactors except boiling reactor, the temperature of the coolant is dependent upon reactor power and coolant flow rate as seen in Eq. (3). If flow rate is constant, temperature will vary directly with reactor power. If reactor power is constant, temperature will vary inversely with flow rate.

Since the rate of heat generation is ideally proportional to the volume of the fuel, it is far more convenient to use volumetric heat generation rate rather than the overall rate of heat generation. The average value of volumetric heat generation may be given by,

$$\dot{q}'''_{avg} = \frac{\dot{q}}{V_F} \quad (6)$$

In case of TRIGA Mark II research reactor established in Atomic Energy Research Establishment (AERE) under the Bangladesh Atomic Energy Commission, the average volumetric heat generation rate is found to be ~75.8 MW/m^3.

The volumetric heat generation rate at any axial location is given by,

$$\dot{q}''' = \dot{q}_{max}'''\cos\left(\frac{\pi z}{H}\right) \quad (7)$$

Here z is the location at axial direction. Volumetric heat generation rate at a specific location of the fuel element is proportional to the neutron flux at that location. Since neutron flux varies in the axial direction of the fuel rod, volumetric heat generation rate also varies in the axial direction. The expression for volumetric heat generation rate related to neutron flux is presented in equation (8).

$$\dot{q}'''(z) = \dot{q}'''_{avg}\frac{\varphi(z)}{\varphi_{avg}} \quad (8)$$

Here is the volumetric heat generation rate at any axial distance z and is neutron flux at that location. Also, heat flux is proportional to volumetric heat generation. As a result, the distribution of neutron flux inside a reactor inside a specific rod should mimic the neutron flux distribution of the same fuel rod. Fig.3 shows the heat flux distribution for the "hot rod" of the TRIGA Mark II research reactor in AERE [31].

In order to obtain the temperature inside a fuel rod or cladding at a specific location at a given time, it is necessary to apply the three-dimensional unsteady-state energy equation with internal heat generation, which is given by,

$$\frac{1}{r}\frac{\partial}{\partial r}\left(kr\frac{\partial T}{\partial r}\right) + \frac{1}{r^2}\frac{\partial}{\partial \theta}\left(k\frac{\partial T}{\partial \theta}\right) + \frac{\partial}{\partial z}\left(k\frac{\partial T}{\partial z}\right) + \dot{q}''' = \frac{\partial}{\partial t}\left(\rho C_p T\right) \quad (9)$$

Here T is the local temperature of the solid (fuel or cladding) and ρ and C_p are the density and specific heat capacity of the solid respectively. Also, k is the thermal conductivity (W/m.K) of the element considered. In case of cladding, there is no volumetric heat generation and thus the term will be omitted from equation (9).

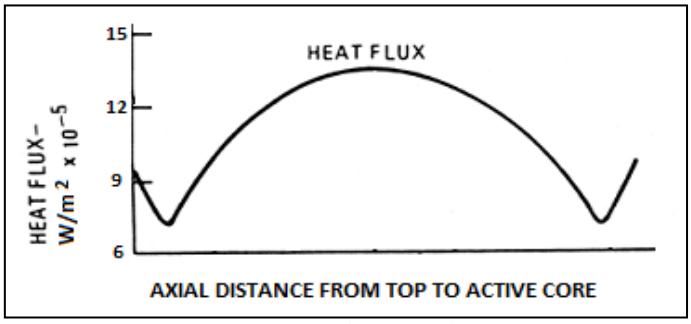

Fig. 3: Heat Flux Distribution Inside the "Hot Rod" in Axial Direction [31].

Fig.4 shows the typical construction of a fuel rod used in TRIGA Mark II research reactor in AERE. The dimension of each component of the fuel rod in two-dimensional coordinate system is shown in Fig.5. The fuel element is Uranium Zirconium Hydride ($U_{0.3}ZrH_{1.6}$), which has a much higher thermal conductivity compared to conventional nuclear fuel element i.e. Uranium Oxide (UO_2). The U-235 enrichment of fuel is also higher for research reactors, as stated earlier. It may be noted that the active length of the fuel element is 38.1cm. There are graphite layers and stainless steel fittings on both end of the fuel rod, which have no active participation in the nuclear fission reaction. Graphite layers at the two sides act as reflectors.

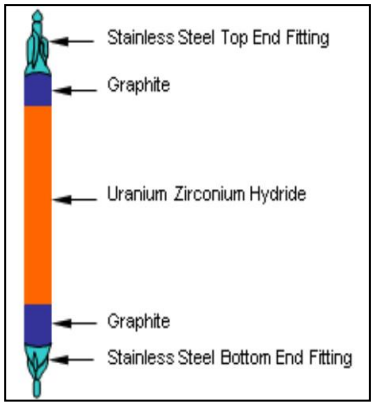

Fig. 4: Typical Construction of A TRIGA Mark II Reactor Fuel Rod [23].

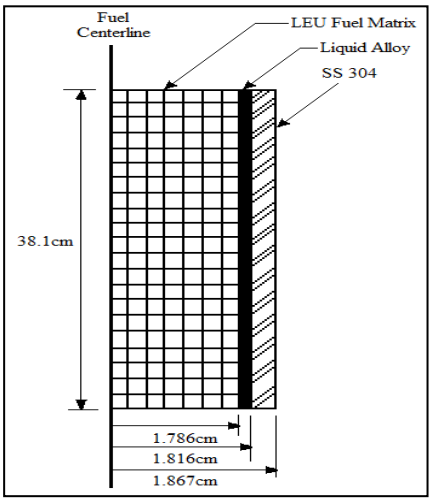

Fig. 5: Dimensions of Different Components of the Fuel Rod in 2-D Co-ordinate System.

The cladding material is made of SS 304 rather than Zircaloy. Another interesting variation in design of the fuel for TRIGA is that the gap between the fuel element and the cladding is filled up by a liquid alloy of Pb-Bi-Sn, which has a melting point lower than 100 ^oC. In case of conventional fuel rods in power reactors, this gap is usually filled up by Helium gas. This modification in design has allowed the fuel centerline temperature to be maintained below 850 ^oC, which is necessary for avoiding fuel swelling and distortion [8]. Different compositions for the Pb-Bi-Sn liquid alloy are available. In this work, it has been assumed that the composition of the liquid alloy is 20% (Bi)-50% (Pb)-30% (Sn).
It may be noted that the gap between the fuel element and cladding is so small that the mode of heat transfer through the liquid alloy is mostly conduction. Therefore, equation (5) should hold for this region too. Of course, heat generation is absent in this region and thus should be omitted from equation (9).
The generated heat in the reactor core must be constantly removed to avoid heating of the fuel rods. TRIGA Mark II research reactor is a pool type reactor, the core being submerged in coolant water. This water, through either natural or forced convection, carries heat away from the system. Therefore, Newton's law of cooling is applicable for the coolant water, which is given by,

$$\dot{q}'' = h\left(T_{clad,out} - T_{\infty}\right) \tag{10}$$

Here, $\dot{q}''$ is heat flux (W/m^2), h is convection heat transfer coefficient (W/m^2.K), $T_{clad,out}$ is cladding outer surface temperature (^oC) and T_{∞} is bulk coolant temperature (^oC).
In order to determine convection heat transfer coefficient, it is necessary to determine the hydrodynamic parameters of the system. To do so, it is much more convenient to apply single channel flow analysis technique rather than performing analysis for the complex geometry of the reactor core structure.

2.3. Simulation techniques

An easy way to comply with the paper formatting requirements is to use this document as a template and simply type your text into it.
Before using Computational Fluid Dynamics (CFD) in analyzing the thermal-hydraulic behavior of a complex flow channel, it is necessary to simplify the geometry of the system. Single channel flow analysis is such a simplified method of analysis. In this method, it is assumed that there is a single flow channel around each fuel rod and each flow channel is unaffected by the adjacent flow channel. As a result, each fuel rod may be analyzed separately without worrying about the existence of the other fuel rods. This assumption reduces the difficulties in the analysis process and also reduces computation time. Fig.6b shows the single annular flow channel considered for this study. Also, a hot rod factor of 1.70 has been considered in this study in order to simulate the results for the fuel rod with highest amount of heat generation i.e. the "hot rod".
The volumetric heat generation rate of reactor fuel element is not constant in the axial direction, as explained in the previous section. However, if it is assumed that there is variation in the axial direction, the CFD model becomes much simpler and should require less computation time. On the other hand, it may also affect the accuracy of the results obtained from simulation. Therefore, a comparative study has been conducted on the two possible methods of simulation; one in which it has been assumed that there is no variation of volumetric heat generation rate in the axial direction and the other one in which there is.
In this work, all the simulations have been conducted in COMSOL Multiphysics, a commercial simulation software that utilizes "Finite Element Method" (FEM). 2-D axi-symmetric model has been selected for conducting the simulation since the fuel rods are cylindrical. Utilizing a 2-D model instead of a 3-D model greatly reduces the computation time.
Fig.6 shows the simulation geometry in which there is no axial variation in heat generation. Since heat generation is uniform throughout the fuel element, it has been assumed that the fuel rod consists of a single, uniform fuel element.

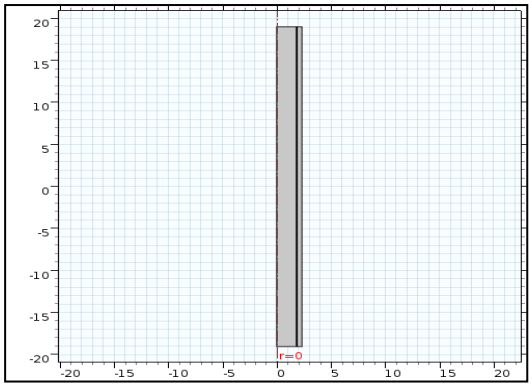

Fig. 6: Simulation Geometry for No Axial Variation in Heat Generation.

Fig.7 shows the mesh distribution for the finite element analysis. Triangular mesh elements have been selected for as they are best suited for the physics behind conjugate heat transfer. From Fig.7, it may be noted that the mesh elements are finer near the outer boundary than the ones near the fuel centerline. The geometry consists of 32833 mesh elements with 3166 boundary elements.

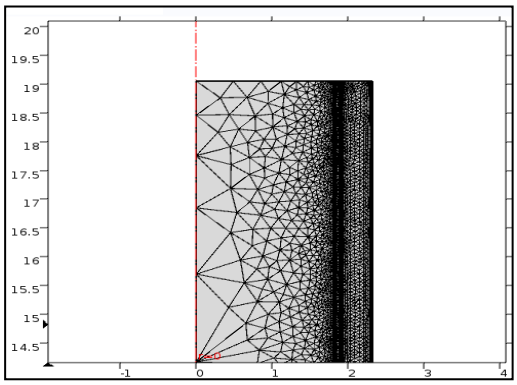

Fig. 7: Mesh Distribution of the Simulation Geometry for No Variation in Heat Generation.

Fig.8 shows the simulation geometry in which there is axial variation in heat generation. In order to accommodate axial variation effect in the simulation model, the fuel element has been divided in 13 regions along the axis. Each element has the same size with different volumetric heat generation rate. The variation in volumetric heat generation follows the pattern observed in Fig.3.
Fig.9 shows the mesh distribution for the finite element analysis of the model that accounts for axial variation in heat generation. From Fig.9, it may be observed that the mesh distribution is almost identical to that observed in Fig.7. A slight variation is observed due to the extra boundaries between the 13 separate regions of the fuel element. The mesh consists of 31469 mesh elements with 3306 boundary elements.
As the maximum coolant flow rate achievable is 13230 liters/min, the velocity of flow through the annular flow is calculated to be 0.207m/s. This flow velocity indicates turbulent flow. Therefore, k-ω turbulence model has been used for simulating the coolant-side thermal-hydraulic parameters. For simulating heat transfer through different regions of the fuel rod, it has been assumed that thermal conductivity, density and specific heat of each material remain constant for all temperatures. Table 1 presents the values of these parameters for different materials of concern.

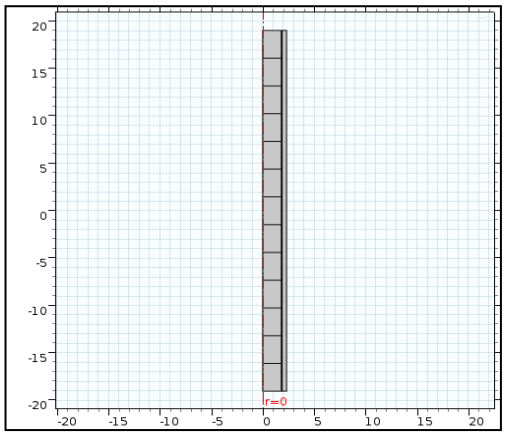

Fig. 8: Simulation Geometry for Axial Variation in Heat Generation.

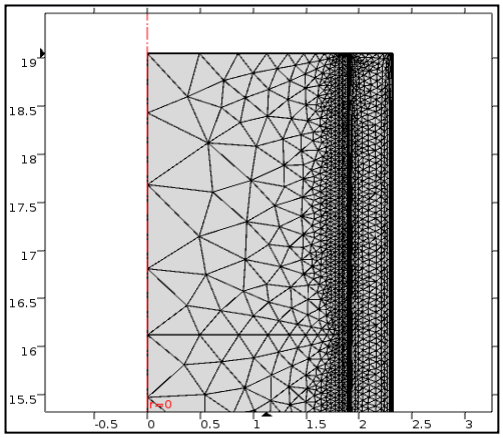

Fig. 9: Mesh Distribution of the Simulation Geometry for Axial Variation in Heat Generation.

Table 1: Properties of Different Materials

Material	k (W/m.K)	ρ (kg/m^3)	C_p (J/kg.K)
$U_{0.3}ZrH_{1.6}$	20 [8]	3715 [8]	-
SS 304	16.2 [32]	7800 [32]	507 [32]
Bi-Pb-Sn (20%-50%-30%)	38.9 [32]	9777 [32]	152.6 [32]

3. Results and discussion

In order to determine the performance of a simulation methodology in predicting a real-life scenario, the simulation results are compared with experimental data for validation. Fig.10 shows the typical pressure drop of the coolant while flowing through the reactor core in a TRIGA Mark II research reactor. From Fig.10, it may be observed that pressure drop is significant only at the entry and exit region of the coolant. There is no noticeable pressure drop while flowing past the fuel cladding surface. This may be due to the length of the fuel rod being so small (only 38.1cm) that it doesn't cause a major pressure drop.

Fig.11 and Fig.12 presents the calculated pressure values at various locations of the flow channel for both the simulation methods. From Fig.11 and Fig.12, it may be observed that the pressure drop across the flow channel due to friction is very small. From single fuel element simulation method, the pressure drop is calculated to be 2.248kPa. For multiple fuel pallet simulation method, pressure drop is found to be 2.261kPa. Both the values are insignificant, similar to the theoretical and real-life values. Therefore, it may be opined that both the simulation methods are capable of predicting pressure drop accurately. It is to be noted that the simulations are in 2-D and thus the losses due to entry and exit region are not considered.

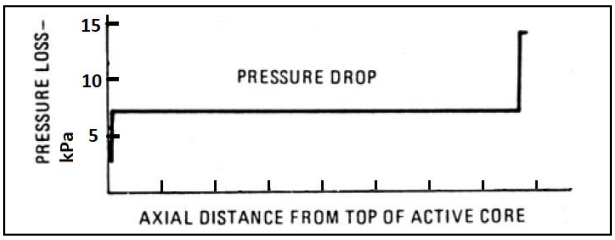

Fig. 10: Pressure Drop Along the Fuel Length for TRIGA Mark II Research Reactor [31].

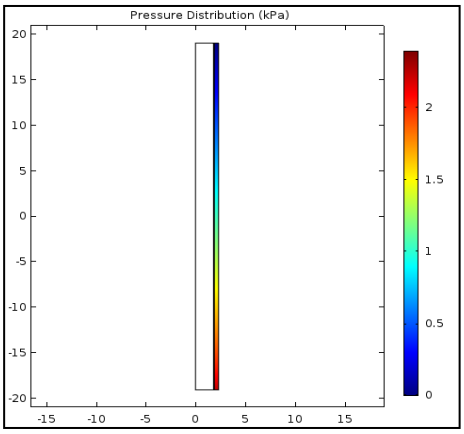

Fig. 11: Pressure Drop in Single Fuel Element Simulation Method.

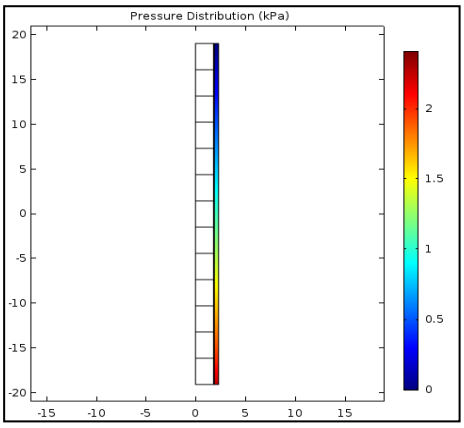

Fig. 12: Pressure Drop in Multiple Fuel Pallet Simulation Method.

Fig.13 shows the variation of temperature inside the fuel element if there is no variation in volumetric heat generation rate along the axis of the fuel. From Fig.13, it may be observed that there is almost no variation in temperature in the axial direction. However, variation in the radial direction is well-defined. The maximum temperature is observed to be along the centerline of the fuel element. The maximum temperature is above 700^{o}C. Fig.14 shows the variation of temperature inside the fuel element if there is variation in volumetric heat generation rate along the axis of the fuel. From Fig.14, it may be observed that there is significant variation in temperature in both axial and radial direction. The maximum temperature is observed to be at the center of the fuel rod, both in axial and radial direction. Also, there is sufficient variation in the temperature distribution compared to that observed in Fig.14. The maximum temperature is just above 750 ^{o}C.

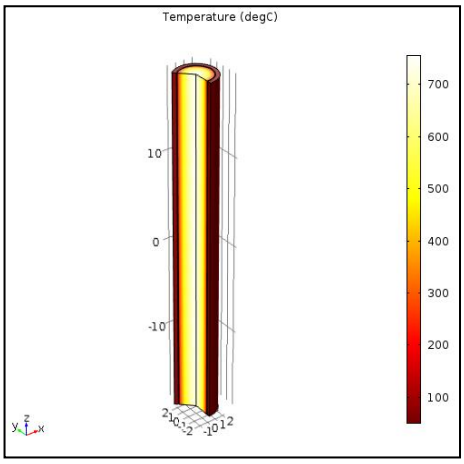

Fig. 13: Temperature Distribution Inside the Fuel Rod for No Axial Variation in Heat Generation Rate.

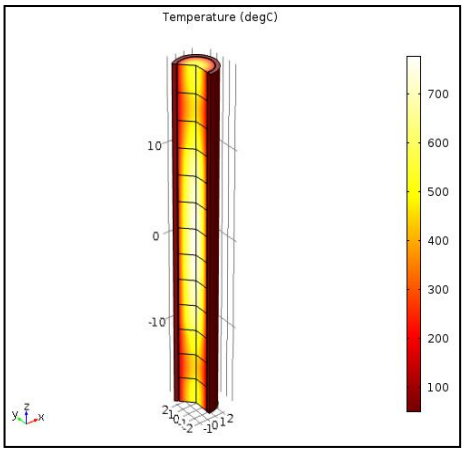

Fig. 14: Temperature Distribution Inside the Fuel Rod for Axial Variation in Heat Generation Rate.

Fig.15 presents the variation of temperature along the axial distance at the fuel centerline obtained from experiments, theoretical calculations and both the simulation methods. From Fig.15, it may be observed that the experimental data are quite different from the values predicted by the theoretical calculations. This is because theoretical calculations don't account for the reflector effects. For single fuel element simulation method, the maximum temperature of fuel centerline obtained is just above 750 ^{o}C, which is just a little lower than the experimental peak value. Also, the temperature is observed to be higher around the mid portion of the fuel rod compared to that at the end of the fuel rod. A similar trend is observed in the experimental data. However, the fuel centerline temperatures at the two ends are somewhat overestimated in the simulation results compared to the experimental data. This is because of the fact that volumetric heat generation has been constant throughout the fuel element, resulting in lesser variation in centerline temperature. On the other hand, there exists variation in heat generation along the axis of the fuel element in real condition and the rate of heat generation is much higher at the middle portion of the fuel rod compared to that at the ends. As a result, centerline temperature is measured to be higher in real-life condition than at the two ends. Since no variation has been accounted for in this simulation technique, the results have somewhat deviated from the actual condition. For multiple fuel pellet simulation method, the maximum temperature of fuel centerline is well above 750 ^{o}C, which is also very close to the experimental value. Also, the pattern of variation in temperature along axial distance is very similar to that observed in the experimental data. Finally, the fuel centerline temperatures at the two ends are found to be almost the same as the experimental values. Since axial variation in volumetric heat generation rate has been accounted for in this simulation technique, the results have been very close to the actual values in almost any location along the centerline.

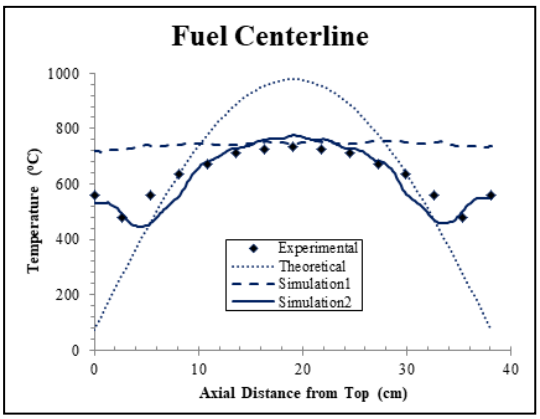

Fig. 15: Variation in Fuel Centerline Temperature for Different Techniques.

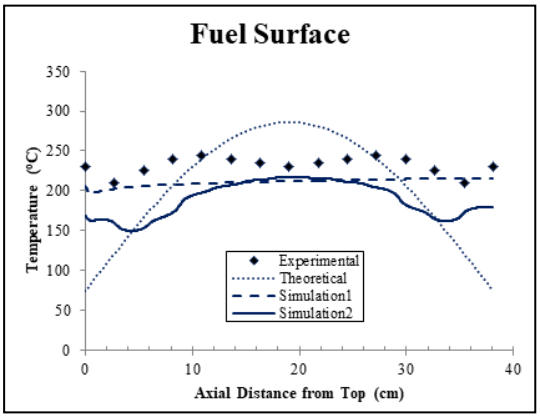

Fig. 16: Variation in Fuel Outer Surface Temperature for Different Techniques.

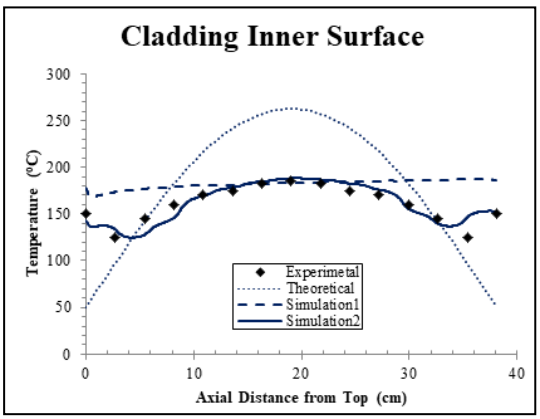

Fig. 17: Variation in Cladding Inner Surface Temperature for Different Techniques.

Fig.16 presents the variation of temperature along the axial distance at the fuel outer surface. From Fig.16, it may be observed that for single fuel element simulation method, fuel surface temperature is observed to be increasing along the length of the fuel rod. This is not the case in real situation. On the other hand, for multiple fuel pellet simulation method, it has been observed that the simulation results have varied a little the experimental data. In the experimental data, there is a decrease in temperature just at the middle portion of the fuel rod. In case of simulation results, however, the maximum temperature is observed to be at the middle portion, just the opposite of the experimental results. The possible reason behind this may be the assumption of constant thermal conductivity throughout the fuel element. In real case, however, there is variation in thermal conductivity of the fuel material with temperature. This issue may be resolved easily by using the actual relationship between thermal conductivity and temperature rather than using a constant value.

Fig.17 presents the variation of temperature along the axial distance at the cladding inner surface. From Fig.17, it may be observed that for single fuel element simulation method, cladding inner surface temperature is observed to be increasing along the length of the fuel rod, just like fuel surface temperature. For multiple fuel pellet simulation method, the simulation results are almost identical to the experimental data.

It may be noted that there are small fluctuations in temperature distribution curves of both the simulation methods. These fluctuations have emerged because of taking finite number of steps (either 1 or 13 values) for volumetric heat generation rate instead of a continuous distribution. This fluctuation may be minimized by increasing the number of steps. However, this may increase computation time and difficulty.

From the above results, it may be stated that the simulation technique that adopts variation in volumetric heat generation rate along the axis of the fuel is sufficient to predict both the maximum temperature of the fuel and the temperature distribution inside the fuel rod with good accuracy. Therefore, this method is highly recommended for analysis. Nevertheless, both the simulation techniques yield better results compared to theoretical analysis.

4. Conclusion

In this work, the feasibility of employing "Single Flow Channel Analysis" technique alongside a CFD simulation tool for analyzing the thermal-hydraulic behavior of a TRIGA Mark II research reactor has been studied. COMSOL Multiphysics has been utilized as the thermal-hydraulic simulation tool. To identify the significance of accommodating axial variation of heat generation rate in the simulation model, two distinct geometries have been introduced. The first geometry consists of a single fuel element which has a volumetric heat generation rate equal to the average value of the same in the TRIGA Mark II research reactor fuel. In the second geometry, the fuel element has been divided into 13 segments, similar to fuel pellets in real situation, each having different values of volumetric heat generation rate. As a result, the second geometry accounted for variation of heat generation in the axial direction. A hot rod factor of 1.70 has been taken for both cases in order to get simulation results for the "hot rod" of the reactor.

Since the fuel rods are arranged in hexagonal array inside the reactor core, the flow sub-channel should have a triangular cross-section. On the other hand, the flow sub-channel should be of annular cross-section for the simulation geometry. Therefore, necessary adjustments are made in the simulation geometry so that the hydraulic diameter remains the same. The flow velocity is taken 0.207m/s since the maximum flow rate is 13230 liters/min. This velocity should induce turbulence flow. Therefore, k-ω turbulence model has been selected for both simulations.

Results show that both the simulation techniques have superior performance compared to theoretical calculations. Again, for the simulation technique with no variation of heat generation rate in axial direction, there is almost no variation in temperature of the fuel centerline in the axial direction. However, the maximum temperature and its location for the fuel centerline are predicted with sufficient accuracy. The fuel centerline temperature has shown a maximum value just above 750 ºC. The values of temperature on fuel centerline at other locations are predicted incorrectly. The simulation technique has also failed to resemble to actual characteristics curves of temperature at the fuel outer surface and cladding inner surface. On the other hand, the simulation technique in which there is variation in heat generation rate along the axis of the fuel, the results are highly similar to the experimental values. The curve representing the fuel centerline temperature is almost identical to the experimental curve. This technique has also predicted the temperature values at other locations inside the fuel rod that are in line with the experimental values.

This work has focused only on identifying the most suitable technique for analyzing the thermal behavior of the fuel rod in TRIGA reactor. This work may be extended to find the behavior of the fuel rod at different rates of heat generation and coolant flow rate. Also, the prospective use of other filler materials in the gap between the fuel and cladding may also be investigated. Finally, the optimum number of segments in the fuel element may be determined in order to obtain best results possible.

Acknowledgement

The authors would like to thank Bangladesh Atomic Energy Commission (BAEC) for providing necessary experimental data for conducting this research. This work has not received any funding or grants from any individual or organization. The authors declare that there is no conflict of interests.

Nomenclature

Symbol	Abbreviation
A	Area (m^2)
C_P	Heat Capacity (J/kg.K)
d	Diameter (m)
f	Friction Factor
g	Gravitational Constant (m/s^2)
H	Height (m)
k	Thermal Conductivity (W/m.K)
$\dot{m}$	Mass Flow Rate (kg/s)
p	Pitch (m)
P	Pressure (Pa)
$\dot{q}$	Linear Heat Generation Rate (W/m)
r	Radius (m)
T	Temperature (K)
ρ	Density (kg/m^3)

References

[1] Anglart H. *Applied Reactor Technology*. 2011.

[2] Glaser A. About the enrichment limit for research reactor conversion: Why 20%? *In: International Meeting on Reduced Enrichment for Research and Test Reactors (hereinafter referred to as RERTR conference)*, Boston 2005 Nov 6.

[3] TRIGA Power System: A Passive Safe Co-Generation Unit for Electric Power and Low Temperature Heat, Small Reactors for Low Temperature Heat Applications, *IAEA-TECDOC-463* (International Atomic Energy Agency, Vienna, 1988) pp. 45-55.

[4] Yamanaka S, Yamada K, Kurosaki K, Uno M, Takeda K, Anada H, Matsuda T, Kobayashi S. Thermal properties of zirconium hydride. *Journal of Nuclear Materials*. 2001;294(1-2):94-8. https://doi.org/10.1016/S0022-3115(01)00457-3.

[5] Toma C, Parvan M, Tuturici IL. Characterization of TRIGA LEU fuel behavior, irradiated in 14 MW core. 2002.

[6] Olander DR, Ng M. Hydride fuel behavior in LWRs. *Journal of nuclear materials*. 2005;346(2-3):98-108. https://doi.org/10.1016/j.jnucmat.2005.05.017.

[7] Wongsawaeng D, Olander D. Liquid-metal bond for LWR fuel rods. *Nuclear Technology*. 2007;159(3):279-91. https://doi.org/10.13182/NT07-A3876.

[8] Olander D, Greenspan E, Garkisch HD, Petrovic B. Uranium–zirconium hydride fuel properties. *Nuclear Engineering and Design*. 2009;239(8):1406-24. https://doi.org/10.1016/j.nucengdes.2009.04.001.

[9] Žerovnik G, Snoj L, Trkov A, Barbot L, Fourmentel D, Villard JF. Measurements of thermal power at the TRIGA Mark II reactor in Ljubljana using multiple detectors. *IEEE Transactions on Nuclear Science*. 2014;61(5):2527-31. https://doi.org/10.1109/TNS.2014.2356014.

[10] Nacir B, Boulaich Y, Chakir E, El Bardouni T, El Bakkari B, El Younoussi C. Safety analysis and optimization of the core fuel reloading for the Moroccan TRIGA Mark-II reactor. *Annals of Nuclear Energy*. 2014; 70:312-6. https://doi.org/10.1016/j.anucene.2013.11.040.

[11] Agbo SA, Ahmed YA, Ewa IO, Jibrin Y. Analysis of Nigeria research reactor-1 thermal power calibration methods. *Nuclear Engineering and Technology*. 2016;48(3):673-83. https://doi.org/10.1016/j.net.2016.01.014.

[12] Štancar Ž, Snoj L. An improved thermal power calibration method at the TRIGA Mark II research reactor. *Nuclear Engineering and*

Design. 2017; 325:78-89. https://doi.org/10.1016/j.nucengdes.2017.10.007.
[13] Cammi A, Ponciroli R, di Tigliole AB, Magrotti G, Prata M, Chiesa D, Previtali E. A zero-dimensional model for simulation of TRIGA Mark II dynamic response. *Progress in Nuclear Energy*. 2013; 68:43-54. https://doi.org/10.1016/j.pnucene.2013.04.002.
[14] El Bakkari B, El Bardouni T, Nacir B, El Younoussi C, Boulaich Y, Boukhal H, Zoubair M. Fuel burnup analysis for the Moroccan TRIGA research reactor. *Annals of Nuclear Energy*. 2013; 51:112-9. https://doi.org/10.1016/j.anucene.2012.07.030.
[15] Türkmen M, Çolak Ü. Analysis of ITU TRIGA Mark II research reactor using Monte Carlo method. *Progress in Nuclear Energy*. 2014; 77:152-9. https://doi.org/10.1016/j.pnucene.2014.06.015.
[16] Coban R. Power level control of the TRIGA Mark-II research reactor using the multifeedback layer neural network and the particle swarm optimization. *Annals of Nuclear Energy*. 2014; 69:260-6. https://doi.org/10.1016/j.anucene.2014.02.019.
[17] Alloni D, di Tigliole AB, Cammi A, Chiesa D, Clemenza M, Magrotti G, Pattavina L, Pozzi S, Prata M, Previtali E, Salvini A. Final characterization of the first critical configuration for the TRIGA Mark II reactor of the University of Pavia using the Monte Carlo code MCNP. *Progress in Nuclear Energy*. 2014; 74:129-35. https://doi.org/10.1016/j.pnucene.2014.02.022.
[18] Henry R, Tiselj I, Snoj L. Analysis of JSI TRIGA MARK II reactor physical parameters calculated with TRIPOLI and MCNP. *Applied radiation and isotopes*. 2015; 97:140-8. https://doi.org/10.1016/j.apradiso.2014.12.017.
[19] Mghar M, Chetaine A, Darif A. Calculation of kinetic parameters of the Moroccan TRIGA Mark-II reactor using the Monte Carlo code MCNP. *Advances in Applied Physics*. 2015;3(1):1-8. https://doi.org/10.12988/aap.2015.531.
[20] Cammi A, Zanetti M, Chiesa D, Clemenza M, Pozzi S, Previtali E, Sisti M, Magrotti G, Prata M, Salvini A. Characterization of the TRIGA Mark II reactor full-power steady state. *Nuclear Engineering and Design*. 2016; 300:308-21. https://doi.org/10.1016/j.nucengdes.2016.01.026.
[21] Ćalić D, Žerovnik G, Trkov A, Snoj L. Validation of the Serpent 2 code on TRIGA Mark II benchmark experiments. *Applied Radiation and Isotopes*. 2016; 107:165-70. https://doi.org/10.1016/j.apradiso.2015.10.022.
[22] Henry R, Tiselj I, Snoj L. CFD/Monte-Carlo neutron transport coupling scheme, application *to TRIGA reactor*. *Annals of Nuclear Energy*. 2017; 110:36-47. https://doi.org/10.1016/j.anucene.2017.06.018.
[23] Manual for Description of the BAEC TRIGA Research Reactor. Bangladesh Atomic Energy Commission, 2012.
[24] Lyric ZI, Mahmood MS, Motalab MA, Khan JH. Optimum burnup of BAEC TRIGA research reactor. *Annals of Nuclear Energy*. 2013; 55:225-9. https://doi.org/10.1016/j.anucene.2012.12.019.
[25] Khan MJ, Sarker MM, Islam SM. Analysis of kinetic parameters of 3 MW TRIGA Mark-II research reactor using the SRAC2006 code system. *Annals of Nuclear Energy*. 2013; 60:181-6. https://doi.org/10.1016/j.anucene.2013.05.009.
[26] Salam MA, Soner MA, Sarder MA, Haque A, Uddin MM, Sarker MM, Islam SM. Measurement of control rod reactivity and shut down margin of 3 MW TRIGA Mark-II research reactor using analogue and digital I&C system. *Annals of Nuclear Energy*. 2014; 68:257-61. https://doi.org/10.1016/j.anucene.2014.01.030.
[27] Rahman MM, Akond MA, Basher MK, Huda MQ. Steady-state thermal-hydraulic analysis of TRIGA research reactor. *World Journal of Nuclear Science and Technology*. 2014;4(02):81. https://doi.org/10.4236/wjnst.2014.42013.
[28] Salam MA, Soner MA, Sarder MA, Haque A, Uddin MM, Rahman A, Rahman MM, Sarkar MM, Islam SM. Measurement of neutronic safety parameters of the 3 MW TRIGA Mark-II research reactor. *Progress in Nuclear Energy*. 2014; 74:160-5. https://doi.org/10.1016/j.pnucene.2014.02.025.
[29] Hosan MI, Soner MA, Kabir KA, Salam MA, Huq MF. Study on neutronic safety parameters of BAEC TRIGA research reactor. *Annals of Nuclear Energy*. 2015; 80:447-50. https://doi.org/10.1016/j.anucene.2015.02.031.
[30] Hoq MA, Soner MM, Rahman A, Salam MA, Islam SM. Estimation of 41Ar activity concentration and release rate from the TRIGA Mark-II research reactor. *Journal of environmental radioactivity*. 2016; 153:68-72. https://doi.org/10.1016/j.jenvrad.2015.12.005.
[31] 3MW TRIGA-Mark-II Research Reactor's Safety Analysis Report, Bangladesh Atomic Energy Commission, 1986, General Atomics, USA.
[32] Thermal properties of metals, metallic elements and alloys. Available online: https://www.engineeringtoolbox.com/thermal-conductivity-metals-d_858.html.